

CONTRASTIVE REPRESENTATION LEARNING FOR ACOUSTIC PARAMETER ESTIMATION

Philipp Götz¹, Cagdas Tuna², Andreas Walther², Emanuel A. P. Habets¹

¹International Audio Laboratories Erlangen[†], Germany.

²Fraunhofer Institute for Integrated Circuits IIS, Erlangen, Germany.

ABSTRACT

A study is presented in which a contrastive learning approach is used to extract low-dimensional representations of the acoustic environment from single-channel, reverberant speech signals. Convolution of room impulse responses (RIRs) with anechoic source signals is leveraged as a data augmentation technique that offers considerable flexibility in the design of the upstream task. We evaluate the embeddings across three different downstream tasks, which include the regression of acoustic parameters reverberation time RT_{60} and clarity index C_{50} , and the classification into small and large rooms. We demonstrate that the learned representations generalize well to unseen data and achieve similar performance compared to a fully-supervised baseline.

Index Terms— Contrastive learning, acoustic scene analysis, audio data augmentation

1. INTRODUCTION

Drawing conclusions about the environmental context from the analysis of an audio recording is a central challenge in acoustic scene analysis (ASA) [1]. Within this field of research, there is a wide range of tasks, such as environment classification [2] or sound event detection [3], whose solutions advance the state-of-the-art in applications such as hearing aid technology [4], audio forensics [5, 6] or robot audition [7]. In some scenarios, a short audio segment is attributed to a single environmental class, i.e., where the particular sample was recorded [8]. In other cases, an audio segment is subject to a time-dependent decomposition into the different contributing sound source types [9]. Apart from such classification tasks, there are scenarios where a regression of room-acoustic parameters, such as reverberation time RT_{60} [10] or clarity index C_{50} [11], or geometric properties, like room volume [12], is performed.

A common characteristic in many ASA problems is the highly variant nature of the observed signals. Originating from real-world environments, they contain intricate mixtures of a wide range of non-stationary sound sources, and may vary significantly in duration. Therefore, it may be desirable to represent an acquired signal from an unknown acoustic environment by a fixed-size embedding that captures the information of interest, while remaining invariant to irrelevant factors. A similar challenge is encountered in text-independent speaker verification [13, 14], where the identity of a person is established, regardless of the particular utterance and the underlying acoustic conditions. Conversely, in the presented study, we aim to extract from a reverberant speech signal a low-dimensional

representation of the underlying room-acoustic conditions, independent of the speaker’s identity or the uttered words. This objective is closely related to acoustic matching [15], where a reverberant input signal is processed to sound as if it was recorded in different surroundings. This is achieved by matching the source-independent latent representations of the source and target channels and reconstructing the transformed output signal. While acoustic matching is concerned with generating perceptually plausible signals, our focus is the representation of physically relevant parameters in an embedding from which we extract information about the environment.

A central concept of contrastive representation learning [16] is the definition of semantic similarity (positive/negative) between input samples, as it forms the basis of the discrimination task and represents an upstream design criterion that directly determines which information is encoded in the embedding space. This may include position-independent environmental features, such as room volume or reverberation time, or position-dependent quantities like source-receiver distance or direct-to-reverberant ratio. In the present work, we assume reverberant speech samples that share the same acoustic impulse response but contain different speech signals to form a positive set. In other words, we leverage convolution with anechoic speech recordings as a data augmentation technique and train a softmax classifier to identify samples that share the same acoustic transmission path. Following this definition, we encourage the encoder network to learn to discriminate between source and channel information. While this proposed concept of similarity forms the basis of the presented work, the authors note that this definition can be freely extended to other criteria. For this purpose, we test the hypothesis that the consideration of different RIRs from the same room as one class should induce a reduction in downstream performance in position-dependent tasks, e.g., C_{50} estimation, while improving accuracy in position-independent tasks, such as volume classification or RT_{60} estimation.

2. PROBLEM FORMULATION

A reverberant signal observed in a room can be defined as the convolution of an anechoic source component, e.g., speech from a human speaker or the sound emitted by a machine, with an RIR, which represents a time-domain description of the acoustic transmission path and contains a wealth of information about the environment. In the presence of uncorrelated, additive sensor noise, this definition can be expressed as:

$$\mathbf{y} = \mathbf{x} * \mathbf{h} + \mathbf{n}, \quad (1)$$

where $(*)$ is the convolution operator and \mathbf{y} , \mathbf{x} , \mathbf{h} and \mathbf{n} denote the observation, the anechoic source signal, the RIR, and the noise signal, respectively. We train an encoder network to extract a low-dimensional representation $\mathbf{e} \in \mathbb{R}^{64}$ from the input \mathbf{y} , which en-

[†]A joint institution of the Friedrich-Alexander-Universität Erlangen-Nürnberg (FAU) and Fraunhofer IIS.
Corresponding author: philipp.goetz@audiolabs-erlangen.de.

codes only information about the acoustic environment contained in \mathbf{h} and is invariant to the source and noise signals \mathbf{x} and \mathbf{n} , respectively. Once upstream convergence is reached, the learned representation serves as input to a downstream network $D(\mathbf{e})$ that is trained on three separate tasks. The estimation of reverberation time RT_{60} in seconds and clarity index C_{50} in decibels, and a binary classification of the room volume.

3. PROPOSED METHOD

The following section covers the contrastive learning approach, the data generation and batch construction, the considered model architecture and the training procedures.

3.1. Supervised contrastive loss

One of the advantages of unsupervised learning is the ability to make use of the great abundance of unlabelled data by considering the views of any single sample as semantically different to the views of all other samples. However, in the context of contrastive learning, this approach also induces a central drawback in the possibility of false negatives, which ultimately limits the discrimination performance. To avoid this upper bound in the presented work, we exploit label information and apply a supervised contrastive loss [17] to the latent representations of the extracted embeddings. Following [18], we use an additional projection network during upstream training that maps \mathbf{e} to a lower-dimensional latent representation $P(\mathbf{e}) = \mathbf{z} \in \mathbb{R}^{16}$ based on which the contrastive loss is computed. Both, the extracted embeddings and their latent representations are l_2 -normalized, they represent coordinates on the surfaces of hyperspheres, where the contrastive loss optimizes jointly the close alignment of similar samples and the approximately uniform distribution of dissimilar samples [19].

We consider a set \mathcal{B} of N randomly selected RIRs, each augmented with M anechoic speech signals and assigned index $i \in \mathcal{I} \equiv \{1, 2, \dots, MN\}$. For each sample \mathbf{y}_i , the set $\mathcal{A}(i) \equiv \mathcal{I} \setminus \{i\}$ contains the indices of all other members of \mathcal{B} , i.e., all remaining positive and negative samples, with cardinality $|\mathcal{A}| = MN - 1$. Furthermore, for each sample \mathbf{y}_i , we define the set $\mathcal{P}(i) \equiv \{p \in \mathcal{A}(i) \mid \mathbf{y}_p \equiv \mathbf{y}_i\}$ to contain the indices of all positive samples relative to \mathbf{y}_i . Following [17], the supervised contrastive loss is given by:

$$\mathcal{L}_{\text{sup}} = \sum_{i \in \mathcal{I}} \frac{-1}{|\mathcal{P}(i)|} \sum_{p \in \mathcal{P}(i)} \log \frac{\exp(\langle \mathbf{z}_i, \mathbf{z}_p \rangle / \tau)}{\sum_{a \in \mathcal{A}(i)} \exp(\langle \mathbf{z}_i, \mathbf{z}_a \rangle / \tau)}, \quad (2)$$

where the inner product $\langle \cdot, \cdot \rangle$ represents the cosine similarity between two latent vectors and τ is a loss temperature hyperparameter that controls the hardness of the estimated class probabilities and reflects the confidence of the classifier.

3.2. Sampling strategies

For the training of the upstream encoder, we investigate different batch construction policies that relate to the concept of hard sampling [20, 21]. The informal definition of a hard negative sample pair is one that “greatly benefits” the model and is highly informative during training. It may be thought of as two observations that appear very similar, but belong to different classes, and, as such, significantly improve the discrimination ability of the model compared to observations that are easily classified correctly. Translating this definition to our context of acoustic environment embeddings, a hard

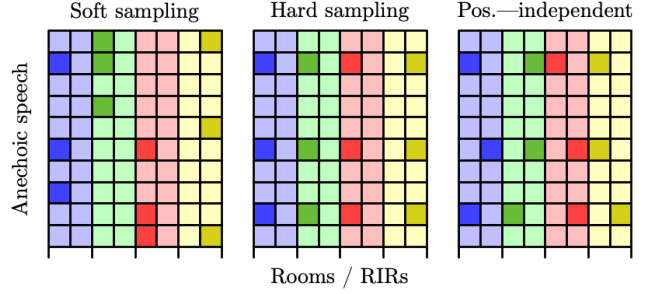


Fig. 1. Illustration of the multiviewed batch construction from a grid dataset: each square represents an individual reverberant input sample, where the row and column indices represent the anechoic speech components and the RIRs, respectively. In this example, two RIRs are simulated for each one of four generated rooms, indicated by the different colors. The batch size is $N = 4$ and the number of different augmentations per sample is $M = 3$.

negative pair consists of two reverberant samples that share the same anechoic speech component but contain different RIRs. As a result, the encoder is presented with data that is semantically different but structurally quite similar, and, as a result, is encouraged to focus on the subtle differences between the two instances of the same source signal, recorded in different environments. In the presented experiments, we train the upstream encoder network with multiviewed batches that contain RIRs augmented with randomly selected speech signals, referred to as *soft sampling*, and with multiviewed batches, in which the selected RIRs share the same speech signal, referred to as *hard sampling*. Furthermore, we extend the latter approach to include the possibility that for each augmentation a different RIR – yet from the same room – is selected. Figure 1 shows an illustrative comparison of the sampling strategies.

3.3. Data generation

In the study, we only consider reverberant speech and assume stationary acoustic conditions with a single source-microphone transmission path. The scope of this study is limited to rectangular rooms, in which RIRs are simulated using the image source implementation of the Python package *pyroomacoustics* [22]. Each room has random length, width and height dimensions in meters, uniformly distributed in the intervals $L \in [3, 10]$, $W \in [3, 10]$ and $H \in [3, 5]$, respectively. The source and the microphone are positioned randomly within the room, while a minimum source-microphone distance and a minimum boundary distance of 50 cm is ensured. Conveniently, the Python package also contains a database of frequency-dependent absorption coefficients for a wide range of construction materials, such as drywall, carpet or glass. Each of the six boundary surfaces in a room is assigned a randomly selected material from this database, which introduces considerable diversity in the data and adds realism to the synthetic RIRs. We make use of the LibriSpeech ASR corpus [23] to construct two fully disjoint datasets. For the upstream training, we simulate RIRs from 64 different rooms and convolve each instance with 128, 32 and 32 four-second segments of anechoic speech to obtain 8192, 2048 and 2048 reverberant speech samples for the training, validation and test subsets, respectively. For the downstream dataset, the same number of samples are generated as in the upstream case, with the difference, that for each sample, an RIR is randomly selected from a data set of 1000 RIRs from 100

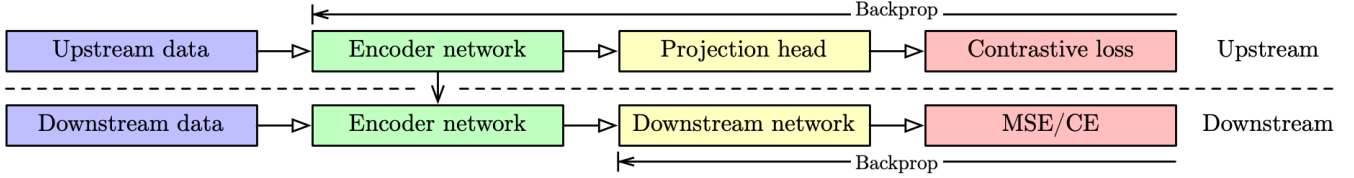


Fig. 2. Illustration of the pipeline. During downstream training and evaluation, the weights of the encoder network are kept fixed, and depending on the target, either mean squared error (RT₆₀ and C₅₀ regression) or cross entropy loss (volume classification) are minimized.

different rooms (10 RIRs per room). The time-domain signals are transformed via STFT to log-magnitude spectrograms, which are subsequently standardized, i.e., they are zero-mean and normalized to unit variance, which accelerates the training process [24]. With a sampling rate of 16 kHz, a window size of 32 samples and a hop size of 16 samples, we choose a high temporal resolution that preserves fine acoustic reflection structures in the input signal, which encode geometric cues from the environment. For the supervised downstream training, we compute the RT₆₀ ground truth based on the energy decay curve [25]. For the binary room volume classification we define a decision boundary of 160 m³ to ensure that each of the two subsets contains an approximately equal number of samples. The distribution of acoustic and geometric parameters in the two data sets is shown in Figure 3.

3.4. Model architectures

We employ a convolutional neural network (CNN) encoder, whose architecture is inspired by prior work in acoustic parameter estimation [10, 26]. The encoder network consists of six convolutional blocks, which extract time-frequency features from the input spectrogram. Each convolutional block comprises a convolution layer, a ReLU activation function and a batch normalization across the convolution channels. The kernel and stride dimensions of all blocks are listed in Table 1. A subsequent dropout regularization prevents overfitting before a fully-connected layer projects the compressed input spectrogram to the fixed-size embedding \mathbf{e} . For all experiments described in this study, we fix the embedding to a vector of length 1024. As mentioned in Sec. 3.1, we use an additional projection network, which produces the latent representation \mathbf{z} and consists of a single hidden layer with 128 neurons and a ReLU activation function. The entire upstream model has a total of 157 k parameters, 2600 of which are part of the projection network.

The downstream model contains the trained upstream encoder

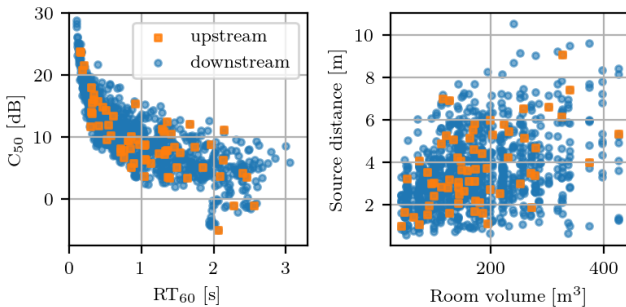


Fig. 3. Distribution of acoustic and geometric parameters in the simulated RIRs of the upstream and downstream data sets.

Layer	1	2	3	4	5	6
Kernel	(1, 4)	(1, 4)	(1, 4)	(1, 4)	(2, 4)	(2, 4)
Stride	(1, 2)	(1, 2)	(1, 2)	(1, 2)	(1, 2)	(2, 2)

Table 1. Parametrization of the six convolutional layers along the dimensions (frequency, time), no zero-padding was used.

and processes the generated embedding by a sequence of two fully-connected layers, each containing 256 neurons. After each projection, a non-linear ReLU activation is applied before the hidden representation is mapped to a particular downstream target. In case of RT₆₀, which only assumes values greater than one, a final ReLU activation is added, for the volume classification, a final softmax function yields the predicted probabilities. The downstream section contains 82.7 k trainable parameters, bringing the total number of the entire model to 237 k parameters.

3.5. Training procedure

Instead of conventional iteration, the upstream data set is randomly sampled, for each forward pass. Thus, we define 128 mini-batches to form an epoch and perform a validation over 32 mini-batches to determine early stoppage. If the validation loss has not decreased for four successive epochs, we abort training and retain the best performing model. The temperature parameter τ in (2) controls the hardness of the estimated class distribution and with it the distinctness of the produced embeddings. We train the upstream encoder at three different temperature coefficients $\tau \in \{0.01, 0.1, 1.0\}$ to investigate the dependence of the learned representations on this hyperparameter. We use a batch size of $N = 24$ with $M = 3$ augmentations per sample, the weights of the model are updated with a learning rate 10^{-3} using the Adam optimizer [27]. The downstream model is trained with every upstream encoder on the three different tasks separately, with a learning rate of 10^{-3} and a batch size of 16. The dropout operation between the convolutional block and the fully-connected layer in the upstream encoder is disabled during downstream training, with an exception for the supervised baseline.

4. EVALUATION

The different sampling strategies and loss temperatures are evaluated based on common performance metrics, which include root-mean-square error (RMSE), Pearson’s correlation coefficient (CORR) and estimation bias for the RT₆₀ and C₅₀ regression, and accuracy (ACC), precision (PR) and recall (RE) for the volume classification.

The results listed in Table 2 show that the representations learned from the contrastive training are highly suitable as input in solving the three downstream tasks. While the results for the different sam-

	τ	SOFT SAMPLING			HARD SAMPLING			POS.-INDEPENDENT		
		RMSE	CORR	BIAS	RMSE	CORR	BIAS	RMSE	CORR	BIAS
RT_{60} [s]	Supervised	0.2228	0.9037	0.0304	0.2228	0.9037	0.0304	0.2228	0.9037	0.0304
	$\tau = 0.01$	0.2699	0.8496	0.0344	0.2369	0.8870	0.0322	0.2146	0.9089	0.0296
	$\tau = 0.1$	0.2345	0.8878	0.0027	0.2426	0.8787	0.0069	0.2217	0.9048	0.0028
	$\tau = 1.0$	0.2500	0.8768	0.0450	0.2770	0.8399	-0.0043	0.2284	0.8937	0.0220
C_{50} [dB]	Supervised	1.9756	0.9241	1.0281	1.9756	0.9241	1.0281	1.9756	0.9241	1.0281
	$\tau = 0.01$	1.7561	0.9208	0.3187	2.0057	0.9227	0.9820	2.2386	0.8908	1.0001
	$\tau = 0.1$	1.8903	0.9223	0.4303	2.0411	0.9142	0.8401	2.0813	0.9063	0.8936
	$\tau = 1.0$	1.7887	0.9181	0.3901	2.0101	0.9032	0.7059	2.3873	0.8597	0.7434
Volume [m ³]		ACC	PR	RE	ACC	PR	RE	ACC	PR	RE
	Supervised	0.6895	0.7066	0.7016	0.6895	0.7066	0.7016	0.6895	0.7066	0.7016
	$\tau = 0.01$	0.6953	0.7146	0.7103	0.7070	0.7252	0.7199	0.7422	0.7320	0.7328
	$\tau = 0.1$	0.7129	0.7241	0.7165	0.6797	0.7014	0.6992	0.7305	0.7586	0.7602
	$\tau = 1.0$	0.7109	0.7376	0.7383	0.6758	0.6943	0.6905	0.6836	0.7024	0.6984

Table 2. Downstream evaluation metrics, the results for the supervised baseline are listed in the column for soft sampling for convenience.

pling strategies and loss temperatures are generally similar, in each of the considered tasks there is a remarkable trend that the models trained with a contrastive loss, without additional fine-tuning, perform at least on par with the fully supervised baseline. In a short experiment, intended as proof of concept, we trained a downstream model that contained an untrained upstream encoder to estimate RT_{60} , and achieved rather large errors of 0.5056s and low correlation coefficients of 0.1993.

We confirm our presumption that the position-independent sampling induces a degradation in performance for the position-dependent C_{50} while proving beneficial for RT_{60} and the room volume classification. This effect is reflected by an increase in RMSE of around 14% for C_{50} and an improvement of the volume classification, from the soft to the position-independent sampling. A possible explanation for this rather moderate change in performance can be found in the ground truth distribution (cf. Fig. 3), which shows the correlation between RT_{60} and C_{50} . If the learned representations are by definition position-independent, the downstream model may infer C_{50} from a well-estimated RT_{60} .

The temperature coefficients used during upstream training do not systematically effect the downstream performance. The results indicate that an optimal choice may depend on the specific task, a further investigation with a finer sampling of the temperature scale may offer additional insights. The effect of hard sampling, as outlined in Sec. 3.2, can be seen in Fig. 4, where we use uniform manifold approximation [28] to qualitatively compare the embeddings of reverberant speech samples from five different rooms. We confirm our hypothesis that sharing the maximum number of speech samples per batch increases the degree of invariance to the source component and results in representations with an increased focus on channel information. Thus, in the case of hard sampling, the discrimination task during upstream training is simplified, as the model does not have to distinguish between different speech samples in addition to the different RIRs. The authors want to emphasize that the metrics results shown in this work represent an exploratory study of our proposed approach to learn room-acoustic representations from reverberant speech signals. We acknowledge that the basic concept of attributing similarity to different observations may be extended to other criteria, depending on the requirements of the representations, which are dictated by the specific downstream task. We hope to inspire further work that adapts our method to suit different requirements.

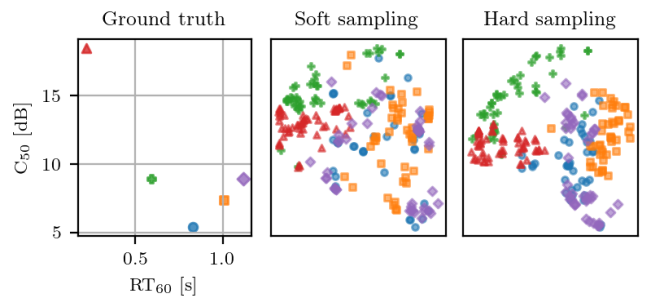


Fig. 4. UMAP plot of the embeddings generated from speech samples in five different rooms. The plot on the left shows the distribution of RT_{60} and C_{50} , the center and right plot show the UMAP projections for the soft and hard sampling strategies. There is a noticeable difference in the degree of the clustering of samples that belong to the same room.

5. CONCLUSION

We present a novel approach to extract low-dimensional representations from reverberant speech signals in a contrastive learning framework. We propose different batch construction policies and demonstrate their effectiveness across three well-known downstream tasks of acoustic parameter estimation and environment classification. By performing at least on par with a fully-supervised baseline, we conclude that our method yields rich representation of the acoustic environment while being invariant to characteristics relating to the source signal.

6. REFERENCES

- [1] Albert S. Bregman, *Auditory scene analysis: The perceptual organization of sound*, MIT press, 1994.
- [2] James Eaton, Nikolay D. Gaubitch, Alastair H. Moore, and Patrick A. Naylor, “Estimation of room acoustic parameters: The ace challenge,” *IEEE/ACM Trans. Audio, Speech, Lang. Process.*, vol. 24, no. 10, pp. 1681–1693, 2016.
- [3] A. Mesaros, T. Heittola, E. Benetos, P. Foster, M. Lagrange,

- T. Virtanen, and M. D. Plumbley, "Detection and classification of acoustic scenes and events: Outcome of the DCASE 2016 challenge," *IEEE/ACM Trans. Audio, Speech, Lang. Process.*, vol. 26, no. 2, pp. 379–393, Feb 2018.
- [4] Simon Doclo, Sharon Gannot, Marc Moonen, Ann Spriet, Simon Haykin, and K.J. Ray Liu, "Acoustic beamforming for hearing aid applications," in *Handbook on array processing and sensor networks*, vol. 9, pp. 269–302. Wiley Hoboken, NJ, USA, 2010.
- [5] Regunathan Radhakrishnan, Ajay Divakaran, and A. Smaragdis, "Audio analysis for surveillance applications," in *Proc. IEEE Workshop on Applications of Signal Processing to Audio and Acoustics (WASPAA)*. IEEE, 2005, pp. 158–161.
- [6] Ghulam Muhammad, Yousef A. Alotaibi, Mansour Alsulaiman, and Mohammad Nurul Huda, "Environment recognition using selected mpeg-7 audio features and mel-frequency cepstral coefficients," in *2010 Fifth international conference on digital telecommunications*. IEEE, 2010, pp. 11–16.
- [7] Selina Chu, Shrikanth Narayanan, C.-C. Jay Kuo, and Maja J. Mataric, "Where am I? Scene recognition for mobile robots using audio features," in *Proc. Intl. Conf. Multimedia and Expo (ICME)*. IEEE, 2006, pp. 885–888.
- [8] Sangwon Suh, Sooyoung Park, Youngho Jeong, and Taejin Lee, "Designing acoustic scene classification models with CNN variants," *Tech. Rep., DCASE2020 Challenge*, 2020.
- [9] Sharath Adavanne, Archontis Politis, Joonas Nikunen, and Tuomas Virtanen, "Sound event localization and detection of overlapping sources using convolutional recurrent neural networks," *IEEE Journal of Selected Topics in Signal Processing*, vol. 13, no. 1, pp. 34–48, 2018.
- [10] Philipp Götz, Cagdas Tuna, Andreas Walther, and Emanuel A.P. Habets, "Blind reverberation time estimation in dynamic acoustic conditions," in *Proc. IEEE Intl. Conf. on Acoustics, Speech and Signal Processing (ICASSP)*. IEEE, 2022, pp. 581–585.
- [11] Hannes Gamper, "Blind C50 estimation from single-channel speech using a convolutional neural network," in *2020 IEEE 22nd International Workshop on Multimedia Signal Processing (MMSP)*. IEEE, 2020, pp. 1–6.
- [12] Andrea F. Genovese, Hannes Gamper, Ville Pulkki, Nikunj Raghuvanshi, and Ivan J. Tashev, "Blind room volume estimation from single-channel noisy speech," in *Proc. IEEE Intl. Conf. on Acoustics, Speech and Signal Processing (ICASSP)*. IEEE, 2019, pp. 231–235.
- [13] Najim Dehak, Patrick J. Kenny, Réda Dehak, Pierre Dumouchel, and Pierre Ouellet, "Front-end factor analysis for speaker verification," *IEEE/ACM Trans. Audio, Speech, Lang. Process.*, vol. 19, no. 4, pp. 788–798, 2010.
- [14] David Snyder, Daniel Garcia-Romero, Gregory Sell, Daniel Povey, and Sanjeev Khudanpur, "X-vectors: Robust DNN embeddings for speaker recognition," in *Proc. IEEE Intl. Conf. on Acoustics, Speech and Signal Processing (ICASSP)*. IEEE, 2018, pp. 5329–5333.
- [15] Jiaqi Su, Zeyu Jin, and Adam Finkelstein, "Acoustic matching by embedding impulse responses," in *Proc. IEEE Intl. Conf. on Acoustics, Speech and Signal Processing (ICASSP)*. IEEE, 2020, pp. 426–430.
- [16] Ashish Jaiswal, Ashwin Ramesh Babu, Mohammad Zaki Zadeh, Debapriya Banerjee, and Fillia Makedon, "A survey on contrastive self-supervised learning," *Technologies*, vol. 9, no. 1, pp. 2, 2020.
- [17] Prannay Khosla, Piotr Teterwak, Chen Wang, Aaron Sarna, Yonglong Tian, Phillip Isola, Aaron Maschinot, Ce Liu, and Dilip Krishnan, "Supervised contrastive learning," *Proc. Neural Information Processing (NIPS)*, vol. 33, pp. 18661–18673, 2020.
- [18] Ting Chen, Simon Kornblith, Mohammad Norouzi, and Geoffrey Hinton, "A simple framework for contrastive learning of visual representations," in *Proc. Intl. Conf. Machine Learning (ICML)*. PMLR, 2020, pp. 1597–1607.
- [19] Tongzhou Wang and Phillip Isola, "Understanding contrastive representation learning through alignment and uniformity on the hypersphere," in *Proc. Intl. Conf. Machine Learning (ICML)*. PMLR, 2020, pp. 9929–9939.
- [20] Joshua Robinson, Ching-Yao Chuang, Suvrit Sra, and Stefanie Jegelka, "Contrastive learning with hard negative samples," *arXiv preprint arXiv:2010.04592*, 2020.
- [21] Yannis Kalantidis, Mert Bulent Sariyildiz, Noe Pion, Philippe Weinzaepfel, and Diane Larlus, "Hard negative mixing for contrastive learning," *Proc. Neural Information Processing (NIPS)*, vol. 33, pp. 21798–21809, 2020.
- [22] Robin Scheibler, Eric Bezzam, and Ivan Dokmanić, "Py-roomacoustics: A python package for audio room simulation and array processing algorithms," in *Proc. IEEE Intl. Conf. on Acoustics, Speech and Signal Processing (ICASSP)*. IEEE, 2018, pp. 351–355.
- [23] Vassil Panayotov, Guoguo Chen, Daniel Povey, and Sanjeev Khudanpur, "Librispeech: an ASR corpus based on public domain audio books," in *Proc. IEEE Intl. Conf. on Acoustics, Speech and Signal Processing (ICASSP)*. IEEE, 2015, pp. 5206–5210.
- [24] Yann A. LeCun, Léon Bottou, Genevieve B. Orr, and Klaus-Robert Müller, "Efficient backprop," in *Neural networks: Tricks of the trade*, pp. 9–48. Springer, 2012.
- [25] Manfred R Schroeder, "New method of measuring reverberation time," *The Journal Acoust. Soc. of America*, vol. 37, no. 6, pp. 1187–1188, 1965.
- [26] Hannes Gamper and Ivan J. Tashev, "Blind reverberation time estimation using a convolutional neural network," in *Proc. Intl. Workshop Acoust. Signal Enhancement (IWAENC)*. IEEE, 2018, pp. 136–140.
- [27] Diederik P. Kingma and Jimmy Ba, "Adam: A method for stochastic optimization," *arXiv preprint arXiv:1412.6980*, 2014.
- [28] Leland McInnes, John Healy, and James Melville, "Umap: Uniform manifold approximation and projection for dimension reduction," *arXiv preprint arXiv:1802.03426*, 2018.